Journal of Systematic Palaeontology **4** (3): 293–306
doi:10.1017/S1477201906001908 Printed in the United Kingdom
Issued 11 August 2006

The fossil record of *Phoberomys pattersoni* Mones 1980 (Mammalia, Rodentia) from Urumaco (Late Miocene, Venezuela), with an analysis of its phylogenetic relationships

Inés Horovitz
Department of Ecology and Evolutionary Biology, 621 Young Drive South, P. O. Box 951606, University of California, Los Angeles, CA 90095-1606, USA

Marcelo R. Sánchez-Villagra
Department of Palaeontology, The Natural History Museum, Cromwell Road, London SW7 5BD, UK

Thomas Martin
Institut für Geologische Wissenschaften, Fachrichtung Paläontologie, Freie Universität Berlin, Malteserstrasse 74-100, 12249 Berlin, Germany

Orangel A. Aguilera
Universidad Nacional Experimental Francisco de Miranda, Centro de Investigaciones en Ciencias Básicas, Complejo Docente Los Perozos, Carretera Variante Sur, Coro, 4101, Estado Falcón, Venezuela and Smithsonian Tropical Research Institute, Center for Tropical Paleoecology and Archeology, Box 2072, Balboa, Republic of Panama

SYNOPSIS An almost complete skeleton of *Phoberomys pattersoni* is reported from the Urumaco Formation in northwestern Venezuela. *Phoberomys* attained the largest body size among known rodents and it lived during the Late Miocene and/or Early Pliocene of Argentina, Brazil and Venezuela. *Phoberomys pattersoni* is probably the second largest species within its genus. The lower molar enamel shows little difference in thickness between the trailing and leading edges in the first and second lophs, whereas in the third loph the trailing edge is much thinner than the leading edge. In the leading edge of the distal loph the enamel consists of two layers, each covering approximately 50% of the entire enamel thickness, one consisting of thick Hunter-Schreger bands inclined 15–20° towards the occlusal surface, the other formed by radial enamel with the prisms inclined towards the occlusal surface. The postcranial skeleton shows a mosaic of unusual features among caviomorphs (e.g. absence of a supratrochlear foramen) and shared conditions (e.g. tuber calcis of the calcaneum that is wider than deeper dorsoventrally) that evolved in parallel in different lineages. The phylogenetic position of *Phoberomys* is determined on the basis of a simultaneous analysis of molecular and morphological data of select rodents. *Phoberomys* appears as the sister group of the Recent genus *Dinomys*. Several derived character conditions are shared with *Dinomys*: presence of a site for attachment for the *m. rectus femoris* on the lateral side of the innominate in the shape of an elongated crest; trochlear ridges of the femur proximally convergent; medial condyle of the femur wider than the lateral one in posterior view; medial ridge of the astragalar trochlea reaches posteriorly further than the lateral one; proximal portion of the coronoid process extends further anteriorly than the medial (and distal) process (or anconeal process). More than one species of *Phoberomys* may be present in the Urumaco Formation.

KEY WORDS Caviomorpha, Hystricomorpha, Neoepiblemidae, *Dinomys*, postcranium, enamel.

Contents

Introduction

South America was inhabited during the Tertiary by rodents with a broad range of body sizes and other physical characteristics. Most notable is the presence of fossils that belonged to species about 10 times larger than the largest living rodent species, *Hydrochoerus hydrochaeris*. Some of the largest rodents belong to the family Neoepiblemidae, and are found in middle Miocene to Pliocene sediments. The genera included in this family are *Phoberomys*, *Neoepiblema* and *Eusigmomys* (Negri & Ferigolo 1999). The genus *Phoberomys* Kraglievich, 1926 is the largest among these and the following species, in order of decreasing size, have been described for it: *P. insolita* Kraglievich, 1940, *P. pattersoni* Mones, 1980, *P. praecursor* Kraglievich, 1932, *P. burmeisteri* Kraglievich, 1926, *P. lozanoi* Kraglievich, 1940, *P. bordasi* Patterson, 1942 and *P. minima* Kraglievich, 1940. The dental sizes of *P. pattersoni* and *P. praecursor* are very close to each other, so the order of decreasing size for these two species given above is tentative, especially considering the poor quality of the dental remains available. Mones (1980) and Sánchez-Villagra *et al.* (2003) incorrectly stated that the mesiodistal length for M3 in *P. lozanoi* was 48 mm, making it the largest species of *Phoberomys*. But this dimension, according to Kraglievich (1940), is actually 34 mm and, therefore, it is among the smaller species of its genus. The species *P. insolita, lozanoi, minima* and *pattersoni*, were originally placed in the genus *Dabbenea* Kraglievich, 1926, however Bondesio & Bocquentin-Villanueva (1988) showed that *Dabbenea* was a synonym of *Phoberomys*.

Most species of *Phoberomys* are known, by and large, from dental remains only. The holotype of *P. burmeisteri* consists of a partial mandible with dentition but several other remains have been attributed to it, including a posterior portion of the skull and three isolated postcranial fragments belonging to femur and tibia. The skeleton we have attributed to *P. pattersoni* is notable because it includes a virtually complete postcranium that was found in articulation with a skull and a partial mandible that were in poor condition, but with a fairly complete dentition (Sánchez-Villagra *et al.* 2003). Since the anatomy of most species is so poorly known and species diagnoses are based mostly on teeth, it is hard to assess if differences in molar sizes are legitimate specific differences or just represent different ontogenetic stages of one another. It is often the case in animals with hypsodont multilaminar teeth that crown size increases with age. Until more cranial and/or postcranial remains are recovered, our understanding of the species diversity of *Phoberomys* will probably remain obscure.

Remains of the various species of *Phoberomys* have been recovered in the Late Miocene and/or Early Pliocene of Argentina (*P. insolita, lozanoi, burmeisteri*, and *praecursor*), Brazil (*P. bordasi*) and Venezuela (*P. pattersoni*). *Phoberomys pattersoni* has been found in the Urumaco Formation, upper Miocene of northwestern Venezuela (Fig. 1). Urumaco is currently a desert, with scarce xerophyitic vegetation and temporary water-courses. It is relatively flat, with small occasional elevations orientated east-west. The sediments are mostly sandstones, limestones and shales (Aguilera 2004). About 8 million years ago, when *Phoberomys* was alive, the area was a coastal wetland with some lagoons of shallow waters, separated from the coast by sandy barriers. The locality in which the most complete specimen of *P. pattersoni* was found (Sánchez-Villagra *et al.* 2003) is 'Tío Gregorio' (11°14′31″N,70°18′40″W: Fig. 1), with strata located at the top of the Urumaco sequence and close stratigraphically to the overlying Codore Formation.

Other large caviomorphs include *Telicomys*, *Tetrastylus*, *Artigasia* and *Eumegamys*, which were smaller than the larger species of *Phoberomys*. The genus *Telicomys* deserves special attention since Nowak (1999) and Savage & Long (1986) have cited it as the largest genus of rodents to ever live. *Telicomys* was created by Kraglievich in 1926, to house two species that Ameghino originally erected as *Tetrastylus giganteus* Ameghino, 1904 and *Tet. gigantissimus* Ameghino, 1908. Ameghino (1908) reported that *Tet. gigantissimus* was the larger of the two and according to Rovereto (1914), the total length of the lower cheek teeth row of

Figure 1 Top: map showing location of 'Tío Gregorio' and 'El Hatillo' localities, Falcón State, northwestern Venezuela. Bottom: view of 'Tío Gregorio', where the skeleton of *Phoberomys pattersoni* (UNEFM-VF-020) was discovered in the upper Miocene Urumaco Formation.

Tel. gigantissimus is 79 mm. Considering that the lower cheek teeth row of *P. pattersoni* is 111.7 mm, the dentition of the largest species of *Telicomys* would have been only about 71% the size of that of *P. pattersoni*.

With the discovery of the skeleton of *P. pattersoni*, it was possible to estimate the body mass for this species in a more reliable way than had been possible before. Sánchez-Villagra *et al.* (2003) conducted analyses that yielded body mass estimates of 436 kg using the humerus and 741 kg using the femur. It is likely that the hindlimbs of *Phoberomys* played a more important role in locomotor propulsion than the forelimbs, therefore we considered the estimate based on the femur to be more reliable (Sánchez-Villagra *et al.* 2003).

We present here some observations of the dental enamel in *P. pattersoni* from an additional specimen we have attributed to this species, a detailed and comparative description of the skeleton mentioned above (Sánchez-Villagra *et al.* 2003), information about some additional remains assignable to *P. pattersoni* or other rodent species discovered in other Urumaco localities and a phylogenetic analysis based on some of its most remarkable postcranial characteristics.

Institutional abbreviations

AMNH, American Museum of Natural History, New York; **CIAAP**, Centro de Investigaciones Antropológicas, Arqueológicas y Paleontológicas, Coro, Venezuela; **LACM**, Natural History Museum of Los Angeles County; **MACN**, Museo Argentino de Ciencias Naturales 'Bernardino Rivadavia', Buenos Aires; **MLP**, Museo de La Plata, Argentina; **UM**, Université II Montpellier; **UNEFM**, Universidad Nacional Experimental Francisco de Miranda, Coro, Venezuela.

Molar enamel

The enamel of a lower m2 deriving from a fragmentary left mandible holding p4–m2 (Fig. 2A) was studied. Koenigswald *et al.* (1994) gave a survey of the schmelzmuster of rootless rodent molars and the following descriptions are based on their terminology. The lower molars of *Phoberomys pattersoni* have three enamel lophs and except for the most distal (third) loph, there is not much difference in enamel thickness between the trailing and leading edges. In the distal loph, the trailing edge is much thinner than the leading edge. Measurements taken from sections vertical to the occlusal surface were 380 μm for the leading edge and 130 μm for the trailing edge, which is a ratio of about 1 : 3 for the distal loph. In the more mesial lophs, the observed enamel thickness is between 360 and 440 μm in both leading and trailing edges.

In the leading edge of the distal (third) loph, the enamel consists of two layers, each covering approximately 50% of the entire enamel thickness (Fig. 2C). The layer adjacent to the cementum that faces in the mesial direction and represents the push-side during mastication, consists of thick Hunter–Schreger bands (HSB) that are inclined 15–20° towards the occlusal surface. The distal portion of the leading edge (pull side during mastication) is formed by radial enamel with the prisms inclined towards the occlusal surface.

The trailing edge of the distal loph that comprises only one third of the thickness of the leading edge, consists of a single layer with thick HSB (Fig. 2D). HSB arrangement is somewhat irregular and the interprismatic matrix (IPM) runs at an acute angle to the prism long axes. This schmelzmuster is the result of a reduction of the internal layer of radial enamel that is present in the trailing edges of the first and second lophs. In the trailing edge of the precedent (second) loph (Fig. 2B), the arrangement of enamel layers is reversed compared to the leading edge of the third loph: the push side, that faces mesially and lies adjacent to the dentine, consists of radial enamel, while the pull side is formed by irregular, thick HSB. The ratio between both layers is 60% (radial enamel) to 40% (HSB).

Postcranial skeleton

Atlas

In dorsal view, two very large lateral vertebral (=alar) foramina can be seen (Fig. 3). The specimen is compressed and the articular surfaces are deformed. Several other vertebrae were preserved but they are in such poor condition that their original morphology cannot reasonably be reconstructed.

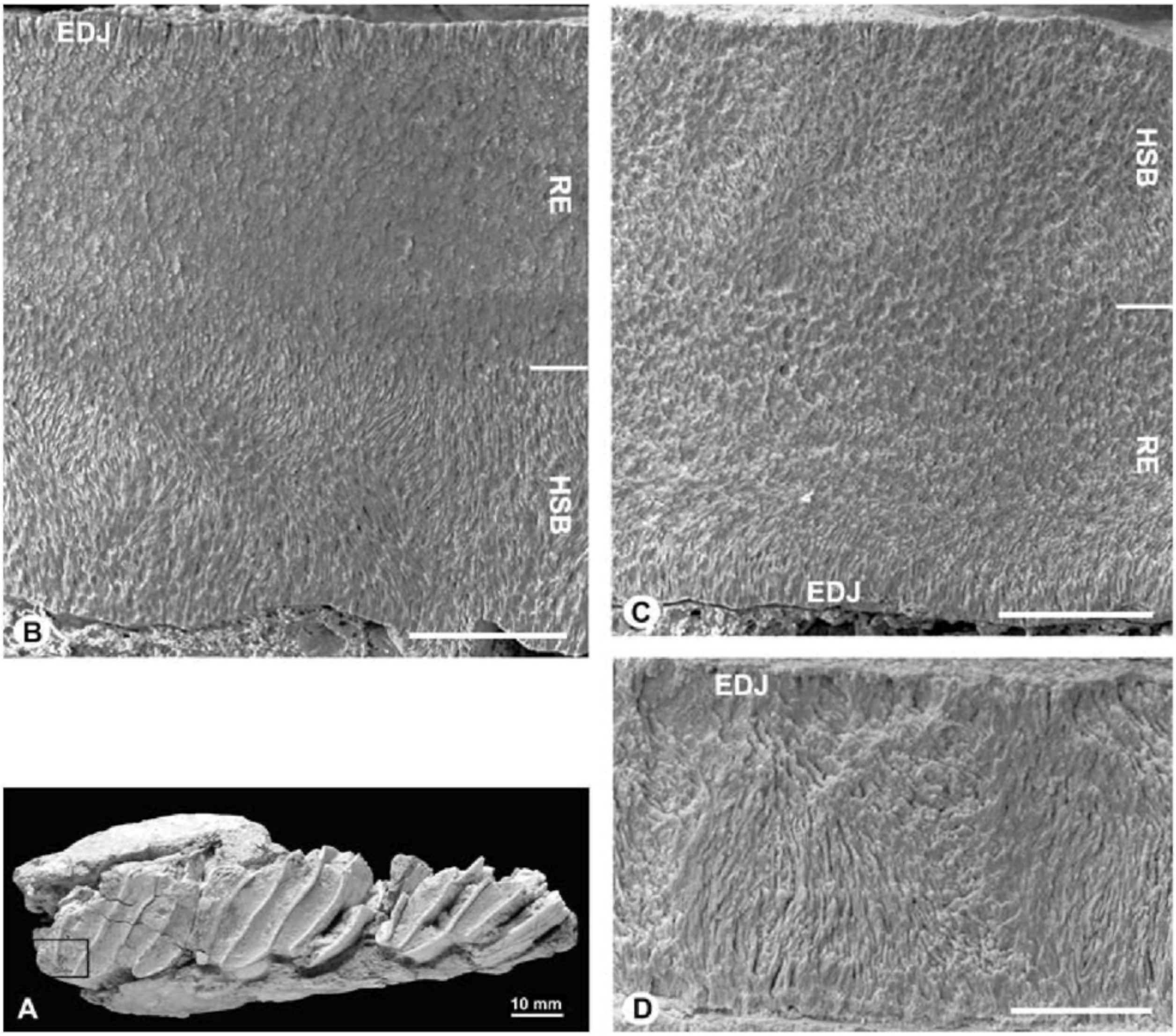

Figure 2 Dentition and molar enamel microstructure of left lower mandible (UNEFM-VF-025) of *Phoberomys pattersoni* from Tío Gregorio (11°14′31″N, 70°18′40″W), Urumaco Formation, Upper Member. **HSB**, Hunter–Schreger bands: **RE**, radial enamel: **EDJ**, enamel–dentine junction. **A**, Occlusal view of p4, m1 and m2. The black rectangle shows the area on m2 from which the enamel has been studied. All enamel sections are longitudinal, the occlusal surface is to the right. **B**, Trailing edge of second enamel loph with EDJ facing in the mesial direction. Adjacent to the EDJ radial enamel, in the lower part of the image there is irregular thick HSB. Scale bar = 100 μm. **C**, Leading edge of third enamel loph with EDJ facing in the distal direction. In the upper part of the image thick HSB is visible, in the lower part, radial enamel can be seen. Scale bar = 100 μm. **D**, Trailing edge of third enamel loph, formed by a single-layered schmelzmuster with irregular, thick HSB. Scale bar = 50 μm.

Humerus

The humerus is known from left and right sides, although the left side is better preserved (Fig. 4). The humeral shaft shows a sigmoid curvature in side view. The greater tubercle and the humeral head are subequal in height, as in the majority of caviomorphs examined. In *Hydrochoerus, Cavia, Dasyprocta, Agouti* and *Dolichotis* the greater tubercle is higher than the humeral head. The deltoid crest is robust and extends from the greater tubercle down to approximately half of the diaphysis, as is the case in most hystricomorph species examined. In *Octodon* and *Dolichotis*, although forming a robust apophysis, the deltoid crest is restricted to the upper third portion of the diaphysis, while in *Cavia, Dasyprocta* and *Aguti* the crest is even more gracile. There are no signs of a teres major tuberosity, but the surface of the humerus in this area is not well preserved, so no final statement about this can be made. The anterior portion of the olecranon fossa forms a crest running proximodistally towards the proximal area of the trochlea. The lateral epicondyle is robust. There is no supratrochlear foramen. All other caviomorphs examined either have this foramen or its presence is intraspecifically variable.

Radius

The proximal end is oval in shape and not circular, the condition of all caviomorphs examined with the sole exception of *Erethizon*. The body is relatively more robust than that

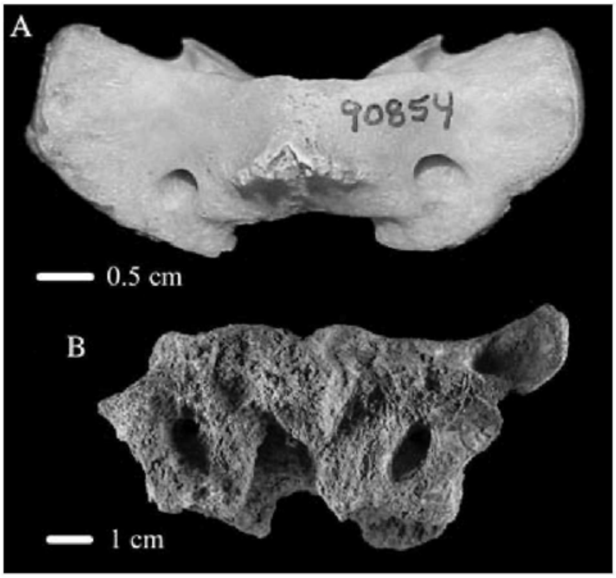

Figure 3 Dorsal views of atlas of **A**, *Dinomys branickii* LACM 90854 and **B**, *Phoberomys pattersoni* UNEFM-VF-020. Posterior ends are at the top.

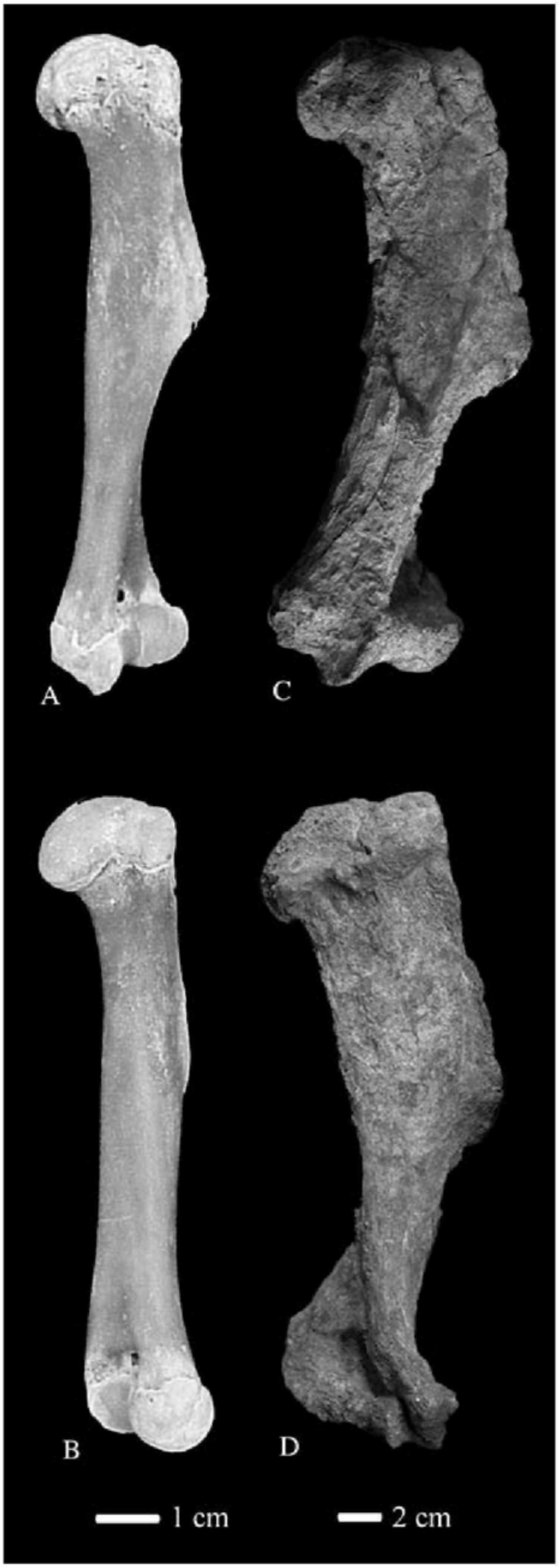

Figure 4 **A–B**, Left humerus of *Dinomys branickii* AMNH 183828 in (**A**) anteromedial and (**B**) posterolateral views. **C–D**, Left humerus of *Phoberomys pattersoni* UNEFM-VF-020 in (**C**) anteromedial and (**D**) posterolateral views.

in *Dinomys* (Fig. 5). In the distal epiphysis, the styloid process is prominent as in *Dinomys*. Poor preservation prevents further description of this bone.

Ulna

The body of the ulna is straight in anterior view (Fig. 6). In posterior view, thickness decreases gradually proximodistally. The ulna is more robust than the radius proximally. The distal end becomes wider as seen in what is preserved of the left ulna. There is a clearly demarcated anconeus process. The olecranon is clearly mediolaterally compressed as in all other caviomorphs examined with the exception of *Erethizon* and *Coendou* where it is relatively short and anteroposteriorly robust as well. As in *Octodon* and as in some specimens of *Dinomys*, *Capromys* and *Proechimys*, the main axis of the olecranon is directed anteriorly in relation to the middle portion of the shaft. In all other caviomorphs examined, the olecranon is either in line with the shaft or directed posteriorly. The distal epiphysis is missing.

Innominate

Most of the left and the dorsal region of the right innominate is preserved. In the left innominate, the acetabular area, the ilium, the pubis and most of the ischium are preserved, except for the ventral branch of the ischium (Fig. 7). The ilium is long and narrow, similar to that of other rodents. The dorsal and ventral edges of the wing are roughly parallel to each other, with the ventral edge curving upwards near the anterior end, as in *Dinomys*, in contrast with *Cavia* where it curves downwards or *Hydrochoerus* where it is almost straight. The caudal ventral iliac spine is weakly defined in *Phoberomys* and *Dinomys*, whereas one is discernible in other caviomorphs such as *Capromys* and *Proechimys*. The caudal dorsal iliac spine is well defined, as in the other rodents.

Figure 5 Right radius in anterior view of **A**, *Dinomys branickii* LACM 90854 and **B**, *Phoberomys pattersoni* UNEFM-VF-020.

There is a strongly defined crest running anteroposteriorly on the lateral side of the ilium that ends posteriorly near the anterior edge of the acetabulum. This crest extends up to the anterior end of the wing. The posterior area of this crest is the site of attachment for the *m. rectus femoris* in living taxa. It usually has the shape of a tuberosity, located just anterior to the acetabulum, as seen in *Hydrochoerus*, *Capromys*, *Proechimys* and *Cavia*, in contrast with the morphology found in *Phoberomys*, which is similar to that of *Dinomys*, in that it has the shape of a crest. In *Phoberomys* the crest displays a prominence towards its posterior end, as it does in *Dinomys*. In *Lagostomus* there is a tuberosity, which is continuous anteriorly with a ridge.

The dorsal ramus of the ischium ends posteriorly in a weak and rounded ischiatic tuberosity. The vertical ramus of the ischium is directed ventrally but with a posterior slant, protruding posteriorly beyond the ischiatic tuberosity. The posteroventral area of the ischium is not preserved.

There is an iliopubic eminence, as in some *Dinomys* specimens. In most other caviomorphs there is occasionally an eminence as well, whereas in *Lagostomus*, there is a large iliopubic process. Part of the ventral pubic–ischiatic ramus is preserved and it shows an anteroposteriorly long surface of contact for the other side of the innominate, as seen in *Dinomys* and the other rodents.

Femur

Both left and right femora are preserved. The left femur suffered postmortem damage, with extensive cracking, deformation, breakage and loss of parts. It is mediolaterally compressed compared to the right femur, which is probably closer to the original morphology. In the right femur, although the parts of the original surface that are preserved are cracked, the surface is smooth and continuous. The description of the femur will, therefore, be based on the right one only (Fig. 8).

The greater trochanter is higher than the head and is a massive process, very wide mediolaterally, protruding laterally beyond the shaft of the femur to a significant degree. In some caviomorphs the greater trochanter does not protrude much laterally at all, such as in *Proechimys*, *Capromys*, *Dinomys* and *Cavia*. In other caviomorphs the greater trochanter protrudes laterally more noticeably and there is a third trochanter distally (e.g. *Hydrochoerus*, *Lagostomus* and other chinchillids and *Dolichotis*). The morphology in *Phoberomys* is different from the latter in that there is no distinct third trochanter and the whole greater trochanter protrudes laterally much more noticeably than in any of those examples.

There is a small lesser trochanter and the intertrochanteric crest does not reach the lesser trochanter distally. The intertrochanteric fossa is not as deep as in other caviomorphs and is limited to the medial side of the greater trochanter, past the level of the lower edge of the head.

The diaphysis is very robust, much more than in any other rodent compared. It displays a small crest on the lateral side, in the distal half of the diaphysis, but not too far from the proximodistal middle. *Hydrochoerus* displays a crest in the same position, whereas *Dinomys* has a prominence in this area, although it is much slighter than in either of the larger taxa.

The trochlea for the patella resembles that of *Dinomys*, where the lateral and medial sides of the facet converge proximally, rather than being almost parallel as in *Hydrochoerus*. The medial edge of this trochlea is considerably raised compared to the lateral one, as can be seen in distal view. It resembles most *Dolichotis* and *Lagostomus* in this regard, although in *Phoberomys* the trochlea is shallower than in either of these examples. There is a sharp contrast between the condition present in *Phoberomys* and *Dinomys*: in the latter the lateral edge is slightly raised with respect to the medial one. In the other rodents examined, both edges were subequal in height although in *Hydrochoerus*, the medial one is slightly more raised than the lateral one.

In posterior view, the medial condyle is wider than the lateral one, contrary to the condition in the capybara. In *Dinomys* both condyles are subequal in width.

Tibia

Both tibiae are preserved almost entirely, except for the distal end of the right one. The proximal end is slightly asymmetrical as in living rodents, with the lateral condyle being wider than the medial one. The proximal end of the tibia is wider

Figure 6 Right (**1 & 2**) and left (**3 & 4**) ulna in (**a**) anterior, (**b**) medial and (**c**) lateral views of (**1 & 3**) *Dinomys branickii* LACM 90854 and (**2 & 4**) *Phoberomys pattersoni* UNEFM-VF-020.

mediolaterally than anteroposteriorly, as in *Dinomys* and the other caviomorphs examined (Fig. 9). In lateral view, the outline of the anterior surface of the tibia shows an angle slightly above the middle, where the distal continuation of the tibial tuberosity ends, separating the proximal portion of the tibia from the distal one. This arrangement is slightly more marked than in *Dinomys* and *Hydrochoerus* for example, where the transition between both areas is more gradual (Fig. 10).

In contrast with both Recent taxa just mentioned, the tibia is very robust. Although the distal end is thinner than the proximal end, the difference is not as marked as in living rodents. The distal end displays the typical posterior process found in all rodents and, apparently, there was no medial malleolus.

Astragalus

The posterior area of the trochlea is not as deep as in *Dinomys* (Fig. 11). In *Phoberomys* the area lateral to the trough is much wider than the medial one, which has a much steeper slope, similar to the condition found in all caviomorphs examined. The neck is relatively shorter than in *Dinomys* and the articular facet for the navicular of *Phoberomys* does not extend dorsally as much as it does in *Dinomys*. In contrast with *Dinomys* and *Hydrochoerus*, the trochlea does not end anteriorly in a ridge on the neck but there is rather a smooth transition between both areas. The head displays a medial surface at an angle from the surface for the navicular, which is facing distally. In modern rodents there is a sesamoid in the medial area which makes contact with the head of the astragalus. This sesamoid is usually very large among caviomorphs and it has a well-defined articular surface for the astragalar head, filling in the gap between the sustentacular facet and the navicular and surrounding the head medioventrally. It is often the case that the head displays a continuous surface for the sustentacular facet, the navicular and the sesamoid. In *Phoberomys* the astragalonavicular facets are continuous and the medial articular area, presumably for a sesamoid, is also continuous with the astragalonavicular

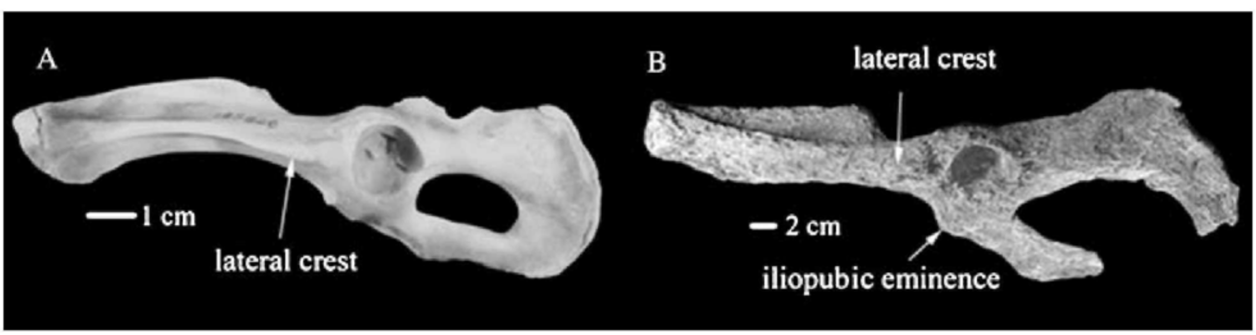

Figure 7 Left innominate bone in lateral view of **A**, *Dinomys branickii* AMNH 183828 and **B**, *Phoberomys pattersoni* UNEFM-VF-020.

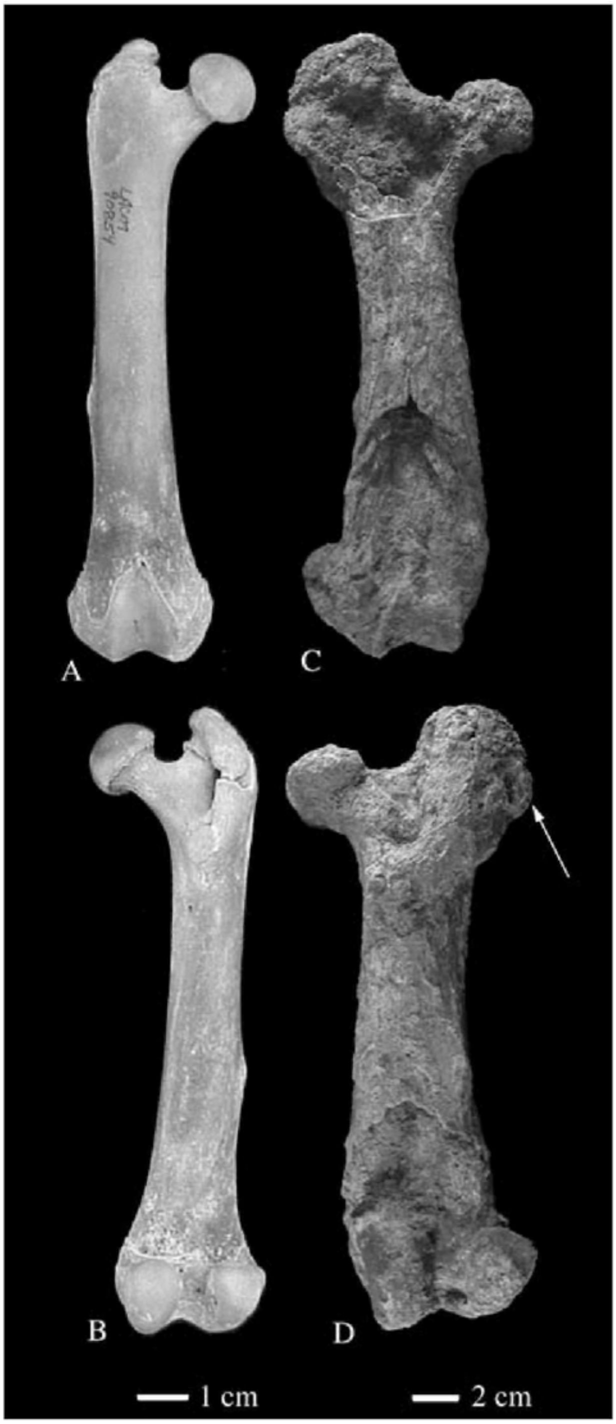

Figure 8 **A–B** Right femur of *Dinomys branickii* LACM 90854 in (**A**) anterior and (**B**) posterior views. **C–D** Right femur of *Phoberomys pattersoni* UNEFM-VF-020 in (**C**) anterior and (**D**) posterior views. Arrrow is pointing at the portion of the greater trochanter that protrudes laterally.

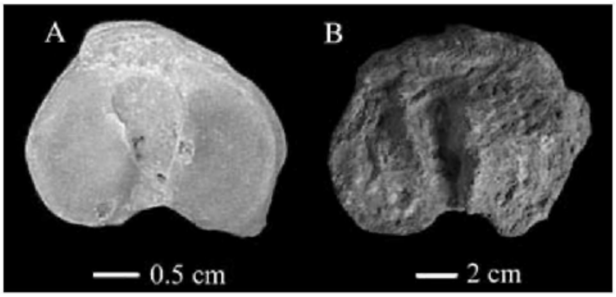

Figure 9 Right tibia in proximal view of (**A**) *Dinomys branickii* LACM 90854 and (**B**) *Phoberomys pattersoni* UNEFM-VF-020. Anterior side is at the top.

Figure 10 Right tibia in lateral view of (**A**) *Dinomys branickii* AMNH 183828 and (**B**) *Phoberomys pattersoni* UNEFM-VF-020. Anterior side is to the right.

facet. This can be seen on the left astragalus but not the right one, the latter being poorly preserved.

The posterior astragalocalcaneal or ectal facet is orientated with its major axis posteromedially to anterolaterally. Although the surface is somewhat damaged, one can still see that it is concave along the same axis, with the concavity increasing towards the posteromedial end.

It is noticeable in ventral view that the medial area of the trochlea reaches further posteriorly than the lateral area, as in *Dinomys* or *Cavia*, and in contrast to *Hydrochoerus*, *Capromys* and *Proechimys*, where they are subequal.

Calcaneum

Both left and right calcanei are preserved, although the left one is more complete (Fig. 12). It is robust and massive. The ectal and sustentacular facets are poorly preserved, making the description of this area or the definition of the borders

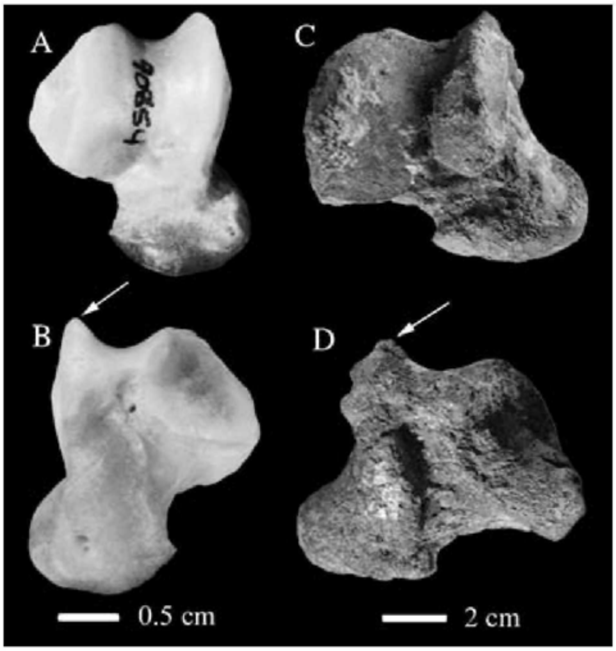

Figure 11 **A–B**, Right astragalus of *Dinomys branickii* LACM 90854 in (**A**) dorsal and (**B**) plantal views. **C–D**, Right astragalus of *Phoberomys pattersoni* UNEFM-VF-020 in (**C**) dorsal and (**D**) plantal views. Arrows are pointing at the medial area of the astragalus that protrudes posteriorly.

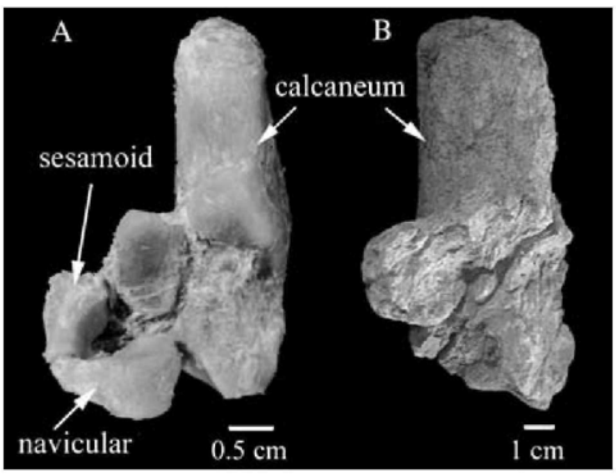

Figure 12 Left calcaneum in dorsal view of (**A**) *Dinomys branickii* LACM 90854 (also showing sesamoid and navicular) and (**B**) *Phoberomys pattersoni* UNEFM-VF-020.

between them impossible. The distal facet for the cuboid is partially visible in dorsal view since, as in other rodents, it folds medially and slightly dorsally.

The tuber calcis is straight and very thick. It is shorter than the main body of the calcaneum. In *Phoberomys*, the tuber calcis is slightly wider than deeper dorsoventrally, as in *Dinomys, Cavia* and *Lagostomus*, and not deeper dorsoventrally as in *Hydrochoerus*, *Erethizon* or *Proechimys*. There is a lateral peroneal tubercle near the anterior end of the calcaneum. The posterior extent of this tubercle is hard to assess because of the bad condition of the specimen, although we do not discard the possibility that it might have extended as a crest possibly reaching the level of the posterior facet, as seen in some *Dinomys* and *Capromys* specimens.

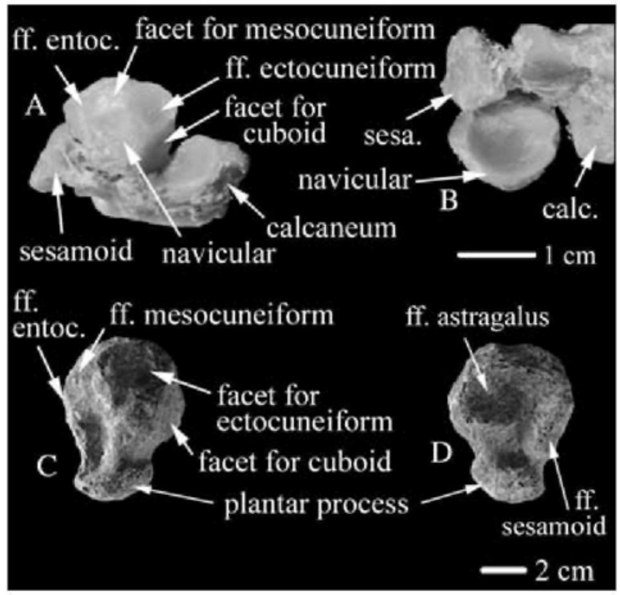

Figure 13 **A–B**, Left navicular of *Dinomys branickii* LACM 90854 in (**A**) distal and (**B**) proximal views (also showing sesamoid and calcaneum). **C–D**, Left navicular of *Phoberomys pattersoni* UNEFM-VF-020 in (**C**) distal and (**D**) proximal views. Abbreviations: ff, facet for; entoc, entocuneiform; sesa, sesamoid; calc, calcaneum.

Navicular and distal elements

Both left and right naviculars are preserved. The navicular displays a prominent plantar process much more prominent than in *Dinomys* (Figs 13A & B). In proximal view there is a large, oval and concave facet for the head of the astragalus (Fig. 13D). The major axis of this facet is mediolateral. Another smaller facet is partially visible in proximal view. This facet would have articulated with a large medial sesamoid. The plantar process is linked to the main body of the navicular by a narrower area, resembling a neck in both proximal and distal views. The navicular displays an approximately round depression in the proximal surface of its neck. In distal view the navicular displays a series of four consecutive facets (Fig. 13C). From medial to lateral these are for the entocuneiform (only slightly visible in this view), mesocuneiform, ectocuneiform (best seen in this view) and cuboid. There is a large dorsoventrally orientated depression in the medial area of the neck, visible in distal view.

Several distal elements including three metatarsals and two phalanges were also recovered, however bad preservation prevented further identification (Fig. 14).

Phylogenetic analysis

Materials and methods

Fourteen postcranial characters scored for a variety of caviomorphs were combined with molecular data collected by

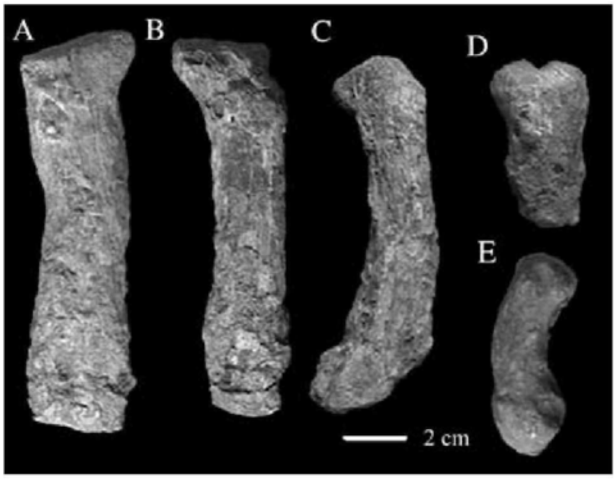

Figure 14 Metatarsals (**A–C**) and phalanges (**D–E**) of *Phoberomys pattersoni* UNEFM-VF-020.

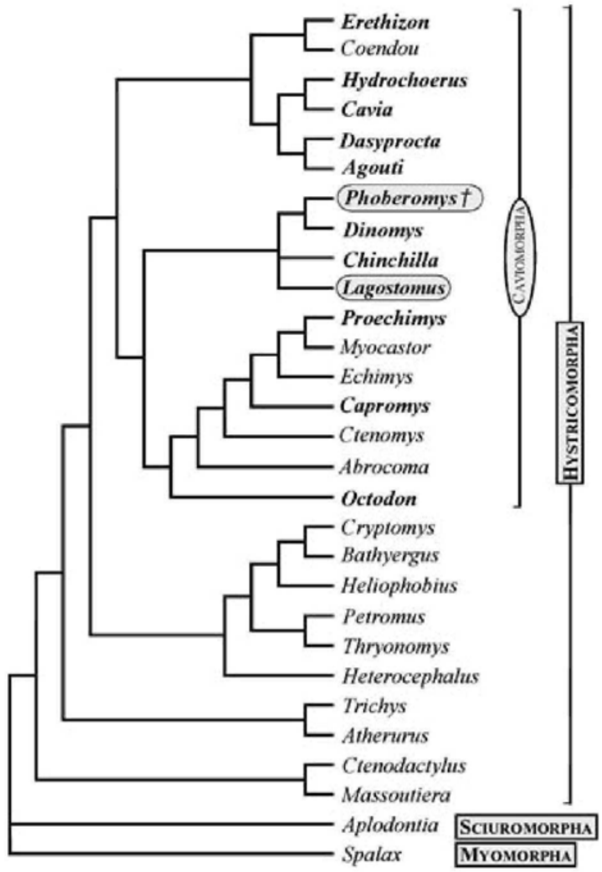

Figure 15 Strict consensus of the two most parsimonious trees resulting from the simultaneous analysis of 14 postcranial characters and DNA sequences from exon 28 of the vWF gene collected by Huchon & Douzery (2001).

Huchon & Douzery (2001) for a simultaneous cladistic analysis. The molecular data set consisted of DNA sequences belonging to exon 28 of the von Willebrand Factor gene (vWF), with a total of 1263 base-pairs, as aligned by the original authors. The alignment was reportedly unequivocal, with one deletion of codon 1 for *Proechimys ori* and one deletion of 10 codons for *Petromus typicus*.

Two species scored for morphological characters only were added to the Huchon & Douzery (2001) data set: *Lagostomus maximus* and *Phoberomys pattersoni*. *Lagostomus* was added to expand on the morphological representation of Chinchillidae, a family that has been suggested as a close relative of our taxon of interest, *Phoberomys*. The morphological characters were first published by Sánchez-Villagra *et al*. (2003), except for character number 14, which is added here (see Appendix 1).

The total number of taxa in the analysis was 29, including one sciuromorph (*Aplodontia rufa* or mountain beaver), one myomorph (*Spalax polonicus* or blind mole rat) and a large variety of hystricomorphs (the remaining 27 taxa), 17 of which were caviomorphs.

The data were analysed using PAUP* version 4.0b10 (Swofford 2002) applying a heuristic search with 200 replications. Wagner trees were obtained with random addition sequence of taxa and they were subject to tree bisection–reconnection. All codon positions and morphological characters were weighted equally and gaps were considered as inapplicable characters. Trees were rooted with *Aplodontia*. A separate analysis was done excluding *Lagostomus* and *Phoberomys* and all 14 morphological characters to compare our maximum parsimony results with those depicted by Huchon & Douzery (2001) based on maximum likelihood.

Results

The cladistic analysis yielded two most parsimonious trees that differed in the position of *Lagostomus maximus*: this species appeared as or either a sister group of *Chinchilla* or as a sister group of the pair *Dinomys–Phoberomys* (Fig. 15; tree length = 1691, consistency index = 0.47, retention index = 0.57, rescaled consistency index = 0.31). Chinchillids have been traditionally grouped on the basis of dental characters whereas this analysis is based solely on postcranial characters alongside the DNA sequences.

Phoberomys appears as the sister group of *Dinomys*, as advanced in a preliminary analysis by Sánchez-Villagra *et al*. (2003). The next closest relative of this pair are the chinchillids (either as a group or as a paraphyletic ladder). Characters supporting a sister group relationship of *Phoberomys* and *Dinomys* are: presence of a site for attachment for the *m. rectus femoris* on the lateral side of the innominate in the shape of an elongated crest, derived from a rounded tuberosity (character 1); the trochlear ridges of the femur are proximally convergent, derived from a condition in which they are parallel to each other (character 2); the medial condyle of the femur is wider than the lateral one in posterior view, derived from the reverse condition (character 4); the medial ridge of the astragalar trochlea reaches posteriorly further than the lateral one, derived from two ridges that are posteriorly subequal (character 6); and finally, the proximal portion of the coronoid process extends further anteriorly than the medial (and distal) process (or anconeal process), derived from a subequal extent (character 13).

The topology of the tree remained stable when morphological data and *Lagostomus* and *Phoberomys* were excluded from the analysis. Note that this topology differs from the maximum likelihood results obtained by Huchon & Douzery (2001) (analysis including all codon positions), in that

Octodon and *Abrocoma* do not appear as sister taxa, *Agouti* and *Dasyprocta* do appear as sister taxa and *Heterocephalus* appears separate from the other bathyergids (*Cryptomys*, *Heliophobius* and *Bathyergus*).

Acknowledgements

We wish to thank Ross MacPhee and an anonymous reviewer for feedback and corrections to our manuscript. Marcia López (CIAAP), Jim Dines (LACM) and S. Jean Spence (AMNH) granted us permission to examine material under their care and Emmanuel Douzery (UM) supplied us with the aligned DNA sequences. Alejandro Kramarz (MACN) and Guiomar Vucetich (MLP) provided information and important literature. This work was supported by the Committee for Research and Exploration of the National Geographic Society (Grant 7600-04 to MRSV).

References

Aguilera, O. A. 2004. *Tesoros Paleontológicos de Venezuela. Urumaco, Patrimonio Natural de la Humanidad*. Editorial Arte: Caracas, 148 pp.

Ameghino, F. 1904. Nuevas especies de mamíferos cretácicos y terciarios de la República Argentina. *Anales de la Sociedad Científica Argentina* **6–8**: 1–142.

— 1908. Las formaciones sedimentarias de la región litoral de Mar del Plata y Chapadmalal. *Anales del Museo Nacional de Buenos Aires* **10** (3): 343–428.

Biknevicius, A. R., McFarlane, D. A. & MacPhee, R. D. E. 1993. Body size in *Amblyrhiza inundata* (Rodentia: Caviomorpha), an extinct megafaunal rodent from the Anguilla Bank, West Indies: estimates and implications. *American Museum Novitates* **3079**: 1–25.

Bondesio, P. & Bocquentin-Villanueva, J. 1988. Novedosos restos de Neoepiblemidae (Rodentia, Hystricognathi) del Mioceno tardío de Venezuela, inferencias paleoambientales. *Ameghiniana* **25** (1): 31–37.

Huchon, D. & Douzery, E. J. P. 2001. From the Old World to the New World: a molecular chronicle of the phylogeny and biogeography of hystricognath rodents. *Molecular Phylogenetics and Evolution* **20** (2): 238–251.

Koenigswald, W. v., Sander, P. M., Leite, M. B., Mörs, T. & Santel, W. 1994. Functional symmetries in the schmelzmuster and morphology of rootless rodent molars. *Zoological Journal of the Linnean Society* **110**: 141–179.

Kraglievich, L. 1926. Los grandes roedores terciarios de la Argentina y sus relaciones con ciertos géneros pleistocenos de las Antillas. *Anales del Museo Nacional de Buenos Aires* **34**: 121–135, pls 1–7.

— 1932. Diagnosis de nuevos géneros y especies de roedores cávidos y eumegámidos de la Argentina. Rectificación genérica de algunas especies conocidas y adiciones al conocimiento de otras. *Anales de la Sociedad Científica Argentina* **64**: 155–181 and 211–237.

— 1940. Los roedores de la familia extinguida Neoepiblemidae. Pp. 741–764 *in* A. J. Torcelli & C. A. Marelli (eds) *Obras en Geología y Paleontología*. Talleres de Impresiones Oficiales: La Plata.

Mones, A. 1980. Un Neoepiblemidae del Plioceno Medio (Formacion Urumaco) de Venezuela (Mammalia: Rodentia: Caviomorpha). *Ameghiniana* **16** (3): 277–279.

Negri, F. R. & Ferigolo, J. 1999. Anatomia craniana de *Neoepiblema ambrosettianus* (Ameghino 1889) (Rodentia, Caviomorpha, Neoepiblemidae) do Mioceno superior-Plioceno, Estado do Acre, Brasil, e revisão das espécies do gênero. *Boletin do Museu Paraense Emílio Goeldi. Serie Ciências da Terra* **11**: 3–81.

Nowak, R. M. 1999. *Walker's Mammals of the World*, 6th edn, Volume 2. Johns Hopkins University Press: Baltimore, 1936 pp.

Patterson, B. 1942. Two Tertiary mammals from northern South America. *American Museum Novitates* **1173**: 1–7.

Rovereto, C. 1914. Los estratos araucanos y sus fósiles. *Anales del Museo Nacional de Buenos Aires* **25**: 1–247.

Sánchez-Villagra, M. R., Aguilera, O. & Horovitz, I. 2003. The anatomy of the world's largest extinct rodent. *Science* **301**: 1708–1710.

Savage, R. J. G. & Long, M. R. 1986. *Mammal Evolution: An Illustrated Guide*. British Museum of Natural History: London, 259 pp.

Swofford, D. 2002. *PAUP* Phylogenetic Analysis using Parsimony (and Other Methods), version 4.0 Beta*. Sinauer Associates: Sunderland.

Appendix 1 Description of characters for phylogenetic analysis and data matrix

1. Pelvis, *m. rectus femoris* attachment (ordered): 0 = non-protruding; 1 = tuberosity; 2 = elongated crest.
2. Femur, trochlear ridges' orientation: 0 = parallel; 1 = convergent proximally.
3. Femur, trochlear ridges' elevation (ordered): 0 = medial raised; 1 = subequal; 2 = lateral raised.
4. Femur, width of condyles in posterior view: 0 = medial condyle wider than lateral condyle; 1 = lateral wider than medial.
5. Astragalus, sustentacular facet, concavity at its posterior end: 0 = flat; 1 = concave.
6. Astragalar trochlea, ridges: 0 = medial ridge reaches posteriorly further than lateral one; 1 = subequal.
7. Calcaneum tuber calcis: 0 = wider than deeper; 1 = deeper than wider.
8. Humerus, supratrochlear foramen: 0 = absent; 1 = present.
9. Humerus, deltoid crest: 0 = strongly built, extending from tuberculum majus down to approximately half of the diaphysis; 1 = deltoid crest forms strong apophysis in the upper third portion of the diaphysis; 2 = slightly built and restricted to uppermost portion of humerus.
10. Humerus, greater tubercle: 0 = higher than humeral head; 1 = subequal in height with the humeral head.
11. Radius, proximal articular surface (*fovea capitis radii*): 0 = anteroposteriorly compressed; 1 = sub-circular.
12. Ulna, main axis of olecranon (additive): 0 = directed anteriorly in relation to medial portion of shaft; 1 = in line with main axis of medial portion of shaft of the ulna; 2 = directed posteriorly in relation to medial portion of shaft.
13. Ulna, anterior extension of anconeal process and coronoid process: 0 = sub-equal; 1 = anconeal process extends further anteriorly.
    This character is correlated with the relative size of the medial coronoid process, the portion of the coronoid process that surrounds medially the head of the radius (the medial coronoid process in these forms corresponds to the coronoid process of humans).
14. Relative length of tibia: 0 = tibia short (no more than 1.69 times longer than the humerus), 1 = tibia long (more than 1.78 times longer than the humerus).

Data matrix

	12345	678910	11121314
Hydrochoerus	10110	11100	0200
Cavia	10100	00120	0200
Erethizon	0010A	11A01	11A0
Chinchilla	10011	11101	0101
Phoberomys	21000	00001	0010
Dinomys	21201	00A01	0A10
Octodon	10110	10111	000?
Capromys	11111	1A101	0A0?
Proechimys	10111	11A01	0A00
Lagostomus	10011	10A01	0101
Dasyprocta	10010	10120	0100
Agouti	10010	11120	011?

Specimens examined are as listed in Sánchez-Villagra *et al.* (2003). A, 0&1; ?, unknown.

Appendix 2 Measurements for *Phoberomys pattersoni* UNEFM-VF-020 and UNEFM-VF-021

As indicated (R, right; L, left), one side or the other was measured depending which one was better preserved.

Specimen UNEFM-VF-020

Length of total lower cheek teeth row (R, L) = 111.7 mm.
Jaw height = 58.3 mm.
Jaw height (including teeth) = 67.5 mm
Measurements of upper teeth (R) are:
P4 : Length = 27.9 mm, width = 20.8 mm.
M1 : Length = 20.6 mm, width = 21.0 mm.
M2 : Length = 18.6 mm, width = 21.0 mm.
M3 : Length = *ca.* 41.0 mm (estimated as posterior portion of tooth is partially broken); width = 20.7 mm.

Humerus: maximum length = 305 mm. Anteroposterior diameter of distal humerus (L) (Biknevicius *et al.* 1993) = 45 mm.

Ulna: olecranon length (L) = 76.2 mm. Length of trochlear notch (L) = 41.7 mm. Length from distal end of trochlear notch to distal end of ulna (L) = 211 mm. Anteroposterior width just distal to trochlear notch (L) = 69.1 mm.

Radius: total length = ca. 299 mm.

Femur: total length (R) = 402 mm. Minimal mediolateral neck width (R) = ca. 44.5 mm. Anteroposterior diameter of proximal femur (R) (Biknevicius *et al.* 1993) = 64.0 mm.

Tibia: length (R) = ca. 377 mm.

Astragalus: trochlear width (R) = 46.8 mm. Maximum length (R) = 78.9 mm. Minimum neck width (R) = 37.1 mm. Head width (R) = 42.7 mm. Plantar width (L) = 61.4 mm. Maximum width of sustentacular facet (L) = 25.8 mm. Maximum width of ectal facet (L) = 28.1 mm. Maximum length of ectal facet (L) = 42.3 mm.

Calcaneus: maximum length = 145.8 mm.

Specimen UNEFM-VF-021 (see Sánchez-Villagra et al. 2003: fig. 1B)

Posterior palate width = 66.0 mm. Width of notch anterior to pterygoids in palate = 33 mm. Distance from top of foramen magnum to nuchal crest = 43.4 mm.

Appendix 3 Additional specimens from Urumaco assignable to *Phoberomys pattersoni* or to related species

Some additional rodent material in the collections of the CIAAP has either never been reported in the literature or been briefly mentioned by Bondesio & Bocquentin-Villanueva (1988) and assigned to *P. pattersoni*. As discussed below, the exact affinities of some of the specimens remain unclear. Future studies will have to elucidate whether they represent morphological and size variation within *P. pattersoni* or rather are examples of other rodent taxa from Urumaco.

cf. *Phoberomys*

Material. CIAAP 1438, see Bondesio & Bocquentin-Villanueva (1988: 33) for a list of materials included in this number, within which M.R.S.V. found the following in the CIAAP collections in January 2004: right and left femora, left humerus, proximal right ulna, proximal radius, left astragalus, two vertebrae, incomplete skull (in two fragments) and right jaw (Figs 16 & 17).

Locality. El Mamón (see Bondesio & Bocquentin-Villanueva 1988), middle member of the Urumaco Formation (Aguilera 2004).

Measurements. Skull dorsal width, posterior to zygomatic arch = 70.6 mm; length of vertical crest running from the bottom of sagittal crest to dorsal border of foramen magnum = 39.6 mm; maximum width of occipital region at the level of the base of paroccipital processes = 82.6 mm; distance between lateral borders of occipital condyles = ca. 51.4 mm (somewhat deformed, so measurement is not exact); length of basioccipital (from suture with basisphenoid to border of foramen magnum) = 41.4 mm; width of ventral side of the skull, at the level of the posterior border of the zygomatic arch's root = 85.5 mm; height of posterior border of dentary (from angle to top of condyle) = 116.9 mm; height of the dentary at the level of m2 = 44.8 mm (without tooth), 50.6 mm (with tooth); length of upper M1 = 16.9 mm; width of upper M1 = 17.00 mm; length of upper M2 = 18.3 mm; width of upper M2 = 18.3 mm; length of right lower m2 = 22.6 mm; width of right lower m2 = 16.5 mm; total length of left humerus = 280 mm; distal left humerus diameter; 35% from distal end (Biknevicius *et al.* 1993) = 26.8 mm; total length of left femur = 360 mm; total length of right femur = 350 mm; proximal right femur diameter, 65% from distal end (Biknevicius *et al.* 1993) = 38.8 mm; proximal left femur diameter, 65% from distal end (Biknevicius *et al.* 1993) = 44.2 mm.

Description. There is a marked sagittal crest in the skull. The boundary between P4 and M1 is exactly at the posterior

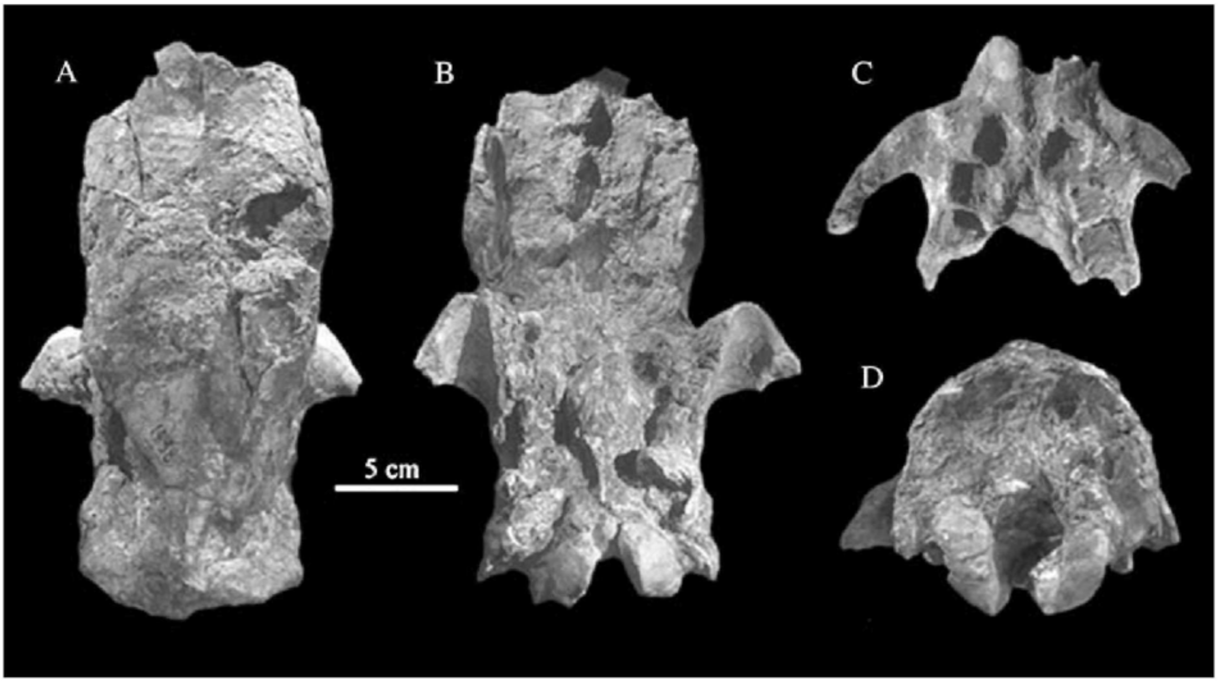

Figure 16 Skull of cf. *Phoberomys* CIAAP 1438 in (**A**) dorsal, (**B–C**) ventral and (**D**) posterior views.

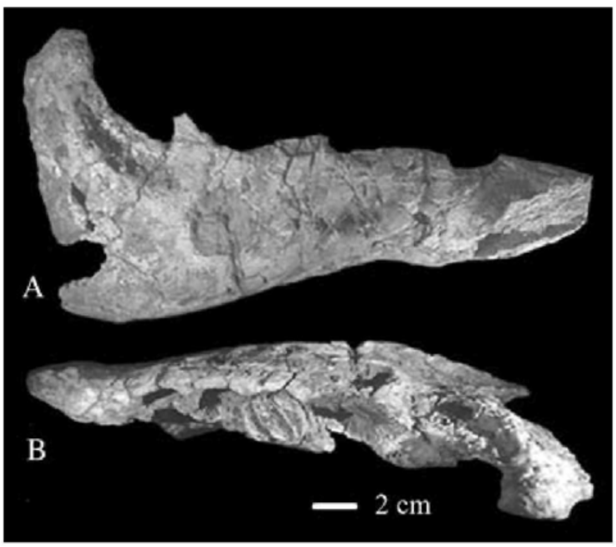

Figure 17 Dentary of cf. *Phoberomys* CIAAP 1438 in (**A**) lateral and (**B**) occlusal views.

border of the anterior beginning of the zygomatic arch. There is a crest running from the bottom of the sagittal crest to the dorsal border of the foramen magnum. The skull preserves the left upper M1-M3. Upper M1 has three prisms and so does the upper M2 (with the same pattern as that illustrated for *Neoepiblema ambrossetianus* by Negri & Ferigolo 1999: fig. 18). The opening of the external auditory meatus does not reach the dorsal-most portion of the skull. The right dentary is almost completely preserved, with the m2 being the only tooth preserved. The humerus has a strong deltoid crest, restricted to the middle area and not reaching the proximal end of the bone (in contrast to *P. pattersoni* UNEFM-VF-020). Both femur and humerus of CIAAP 1438 are more gracile than in UNEFM-VF-020.

Remarks. The specimen CIAAP 1438 was referred by Bondesio & Bocquentin-Villanueva (1988: 33) to *Phoberomys pattersoni*. The skull in CIAAP 1438 is undoubtly smaller than that of *P. pattersoni* UNEFM-VF-021. The presence of a sagittal crest in an animal significantly smaller than UNEFM-VF-020/021 suggests the presence of an additional rodent species in the fauna. The affinities of CIAAP 1438 are difficult to establish in spite of its relative completeness, because of the lack, in this specimen, of a preserved M3. The M3 is of taxonomic importance in this group. Notice also that CIAAP 1438 is reported to have been found at the El Mamón Campo Petrolero locality, in strata belonging to the middle member of the Urumaco Formation (Aguilera 2004). This is stratigraphically much lower than the top of the upper member of the Formation, where UNEFM-VF-020 was found.

cf. *Phoberomys*

Material. CIAAP 441 (left humerus), CIAAP 442 (right femur)

Locality and collection data. Collected by Jean Bocquentin-Villanueva in July 1980 at El Hatillo, Urumaco (Aguilera 2004).

Measurements. Maximum humeral length = 284.8 mm; maximum femoral length = 287.5 mm; femoral length to base of head = ca. 275 mm.

Remarks. A note found at the CIAAP with these specimens states that CIAAP 441 and 442 were found a few metres apart and that, therefore, they might belong to the same individual. We think the latter conclusion is unlikely, given the postcranial proportions of associated skeletons of *Phoberomys* and other rodents found in Urumaco previously. The humeral deltoid crest is very long and extends to the proximal portion of bone, as in *P. pattersoni* UNEFM-VP-020.

cf. *Phoberomys*

MATERIAL. UNEFM-VF-010, right humerus.

LOCALITY. El Hatillo, sector Taparito, Urumaco Formation (11° 14′ 32″ N, 70° 14′ 48″ W).

MEASUREMENTS. Maximum right humerus length = 270 mm; distal humerus diameter, 35% from distal end (Biknevicius *et al.* 1993) = 26 mm.

REMARKS. Because of the lack of associated dental material, it is not possible to assign this material to any species in particular. Because of its morphology it could be *P. pattersoni*, although of smaller size (see UNEFM-VF-026). Notice that the deltoid crest is not continuous with the more proximal portion of the humerus (which is the case in *P. pattersoni* UNEFM-VF-020).

Phoberomys cf. *pattersoni*

MATERIAL. UNEFM-VF-026, fragment of left maxillary containing poorly preserved P4-M3.

LOCALITY. Tío Gregorio (11° 14′ 34 N, 70° 18′ 36 W), a few metres away from where UNEFM-VF025 was found.

MEASUREMENTS. Length of M3 = 29.1 mm; width of M3 = 15.5 mm.

COMMENTS. Assignable to *Phoberomys pattersoni* because of shape and number and arrangement of prisms in M3 (proximity to UNEFM-VF025 supports this assignment). However, it is much smaller than *P. pattersoni* UNEFM-VF-020. This implies that there was either great size dimorphism in this species (as has been suggested for the giant extinct Antillian rodent *Amblyrhiza* by Biknevicius *et al.* (1993)), or that another species besides *P. pattersoni* is represented in Urumaco.

Phoberomys sp.

MATERIAL. CIAAP-1449, isolated dental remains (see Bondesio & Bocquentin-Villanueva 1988).

LOCALITY. 1 km south of Caserío Corralito, near Campo Petrolero El Mamón, Urumaco (Bondesio & Bocquentin Villanueva 1988).

MEASUREMENTS. Length m1 = 18.2 mm; width m1 = 19.0 mm; length P4 = 21.4 mm; width P4 = 16.2 mm; length M1 = 13.5 mm; width M1 = ca. 14.4 mm (estimated); length M2 = 14.9 mm; width M2 = 14.6 mm.

REMARKS. This specimen was assigned to *P. pattersoni* by Bondesio & Bocquentin-Villanueva (1988). Notice however that its dental dimensions are much smaller than those reported by Mones (1980) in the original description of the species.